

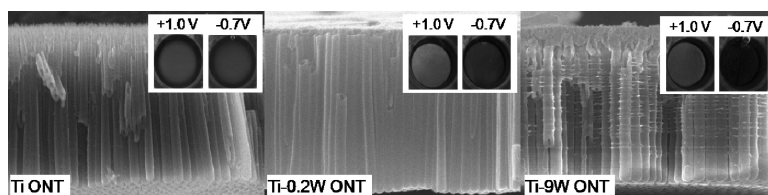
Communication

**TiO<sub>2</sub>/WO<sub>3</sub> Composite Nanotubes by Alloy Anodization:  
 Growth and Enhanced Electrochromic Properties**

Yoon-Chae Nah, Andrei Ghicov, Doohun Kim, Steffen Berger, and Patrik Schmuki

*J. Am. Chem. Soc.*, **2008**, 130 (48), 16154-16155 • DOI: 10.1021/ja807106y • Publication Date (Web): 11 November 2008

Downloaded from <http://pubs.acs.org> on February 8, 2009



**More About This Article**

Additional resources and features associated with this article are available within the HTML version:

- Supporting Information
- Access to high resolution figures
- Links to articles and content related to this article
- Copyright permission to reproduce figures and/or text from this article

[View the Full Text HTML](#)

## TiO<sub>2</sub>–WO<sub>3</sub> Composite Nanotubes by Alloy Anodization: Growth and Enhanced Electrochromic Properties

Yoon-Chae Nah, Andrei Ghicov, Doohun Kim, Steffen Berger, and Patrik Schmuki\*

Department of Materials Science, WW4-LKO, University of Erlangen-Nuremberg, 91058 Erlangen, Germany

Received September 8, 2008; E-mail: schmuki@ww.uni-erlangen.de

Over the past few years, TiO<sub>2</sub> nanotubes (Ti ONTs) have been extensively studied due to their potential application in biomedicine,<sup>1</sup> photocatalysis,<sup>2</sup> photovoltaics,<sup>3</sup> or electrochromic devices.<sup>4</sup> Ti ONTs with different sizes and geometrical shapes could be prepared using various physical and chemical synthesis routes.<sup>5</sup> Among them, a simple electrochemical anodization of a metal in a suitable electrolyte provides the vertically aligned nanotube structure of Ti ONTs with a high surface area.<sup>6</sup> During the anodization process, the electrochemical conditions such as the applied potential, anodization time, and the pH of electrolyte can be used to control the resulting tube diameter, length, and overall morphology.<sup>7</sup>

Incorporation and doping of other species (elements or metal oxides) into TiO<sub>2</sub> have received much attention for improving the electronic or photoelectrochemical characteristics of TiO<sub>2</sub>.<sup>8</sup> Furthermore, the addition of metal oxides to TiO<sub>2</sub> has been reported to improve the photocatalytic or photoelectrolytic activities of TiO<sub>2</sub>.<sup>9</sup> Particularly promising TiO<sub>2</sub> composites may be formed with semiconductive metal oxides such as WO<sub>3</sub>, to enhance either the electronic or the ionic properties of the material. A number of preparation methods have been studied to form active TiO<sub>2</sub>–WO<sub>3</sub> composites such as sol–gel techniques<sup>10</sup> or electrodeposition approaches,<sup>11</sup> which typically are used to build bulk electrodes composed of nanoparticles.

TiO<sub>2</sub> as well as WO<sub>3</sub> belong to the class of oxides that show a strong reversible field-aided ion intercalation behavior. Ions such as H<sup>+</sup> or Li<sup>+</sup> can be comparably easily introduced into these host oxide lattices. This ion insertion is combined with a strong change in the electronic and optical properties of these oxides, and this effect is exploited in electrochromic devices. While Ti ONTs have shown to be excellent candidates for electrochromic applications,<sup>4</sup> their switching voltage as well as contrast at a given voltage is still comparably low. As such, WO<sub>3</sub> is possibly the electrochromic material with the best properties currently known;<sup>12</sup> however, synthesis of robust ordered nanotube layers of WO<sub>3</sub> has not yet been achieved. Anodization of W alone has been reported so far to lead only to disordered or porous structures due to the inherent anodization properties of this material.<sup>13</sup> Here, we demonstrate the first formation and use of ordered tubular TiO<sub>2</sub>–WO<sub>3</sub> structures (Ti–W ONTs) with a high electrochromic contrast. These are formed by electrochemical anodization of TiW alloys and show drastically enhanced intercalation and electrochromic properties that can be achieved already by small amounts of WO<sub>3</sub> in the Ti ONT structure.

Figure 1 presents nanotube layers grown on different substrates [Ti, Ti-0.2 at%W (Ti-0.2W), and Ti-9 at%W (Ti-9W)] by anodization at 120 V in a solution of ethylene glycol with 0.2 M HF. The growth time was controlled to achieve a comparable thickness of the layers; 20 min for Ti, 10 min for Ti-0.2W, and 12 min for Ti-9W. In all cases ordered oxide nanotube layers are obtained with a thickness of 1.1–1.2 μm and an individual tube diameter of 85–95 nm. From the top-view images in Figure 1d–f, it can be seen that on the very top a thin porous layer is present on the nanotubes, which is an initiation layer formed in the very early moments of the anodization process.

Underneath highly defined nanotube layers are present (see also additional images in Figure S1).

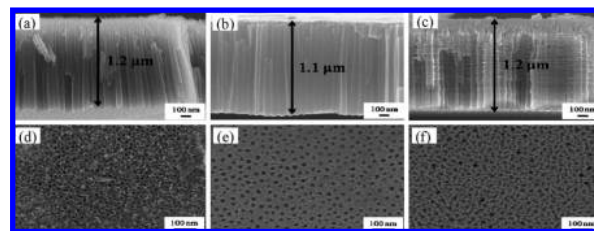


**Figure 1.** Cross-sectional SEM images of ordered oxide nanotube layers grown on (a) Ti, (b) Ti-0.2W, and (c) Ti-9W by anodization in a solution of ethylene glycol with 0.2 M HF at 120 V for 20, 10, and 12 min, respectively, and the corresponding top-view SEM images (d, e, and f).

To explore the ion insertion and electrochromic switching properties of the oxide nanotubes, electrochemical characterization and reflectance measurements were performed. Figure 2a compares the cyclic voltammograms (CVs) of Ti and Ti–W ONTs carried out in 0.1 M HClO<sub>4</sub> solution. The shapes of the CV curves are similar for all samples. The Ti–W ONTs, however, show significantly larger current densities (higher exchanged charge densities) compared to Ti ONTs, which reflects the fact that proton insertion/extraction into the host lattice is facilitated at a given applied potential. Furthermore, the onset potential of the cathodic current for the Ti–W ONTs is strongly shifted in the positive direction compared to the Ti ONTs; that is, insertion can be achieved at a considerably lower applied voltage. The onset potential for WO<sub>3</sub> containing nanotubes, for example, is ~0.2 V lower compared to pure Ti ONTs, even if only 0.2 at% W were present in the base alloy. A further increase in WO<sub>3</sub> content, however, does not change the onset potential. These findings imply that the threshold for cathodic insertion reaction is optimized already at very low amounts of WO<sub>3</sub>.

Figure 2b shows current density response with time when a cycling pulse potential is applied between –0.7 and 1.0 V. The integrated current density with time (charge density) is indicative of protons or electrons incorporated during the reactions. When compared with charge amounts incorporated during cathodic and anodic reactions for Ti and Ti–W ONTs (the inset of Figure 2b), Ti-0.2W and Ti-9W ONTs show much higher values in charge density;  $Q_{\text{cathodic}}$ : –11.6 mC/cm<sup>2</sup>,  $Q_{\text{anodic}}$ : 10.5 for Ti-0.2W ONTs, and  $Q_{\text{cathodic}}$ : –17.3 mC/cm<sup>2</sup>,  $Q_{\text{anodic}}$ : 16.9 mC/cm<sup>2</sup> for Ti-9W ONTs, while  $Q_{\text{cathodic}}$ : –3.4 mC/cm<sup>2</sup>,  $Q_{\text{anodic}}$ : 2.8 mC/cm<sup>2</sup> for Ti ONTs. In other words, for Ti-0.2W ONTs, the amount of charge is ~4 times higher than that of Ti ONTs. (Again, already 0.2 at% of WO<sub>3</sub> changes drastically the properties of the Ti ONTs.) Furthermore, in terms of reversibility, which is estimated by the ratio of charge density ( $Q_{\text{anodic}}/Q_{\text{cathodic}}$ ), the composite nanotubes show clearly better results; 0.91 and 0.98 for Ti-0.2W and Ti-9W ONTs, respectively, while 0.82 for Ti ONTs, indicating that even a higher reversibility of ion movement is provided by small additions of WO<sub>3</sub> into the Ti ONTs.

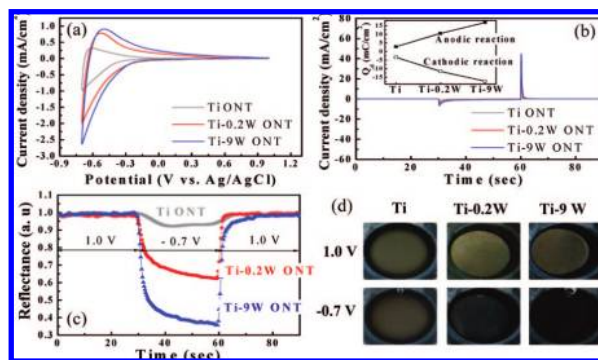


**Figure 2.** (a) Cyclic voltammograms of the oxide nanotube layers on Ti, Ti-0.2W, and Ti-9W performed between  $-0.7$  and  $1.0$  V with a scan rate of  $50$  mV in  $0.1$  M HClO<sub>4</sub> electrolyte; (b) current density–time curves acquired by pulse potential measurement applied between  $-0.7$  and  $1.0$  V with  $30$  s duration; (c) *in situ* reflectance curves of Ti, Ti-0.2W, and Ti-9W ONTs obtained during potential pulsing applied between  $1.0$  and  $-0.7$  V; and (d) optical images of the electrochromic effect of the different nanotube surfaces during polarization cycling between  $1$  and  $-0.7$  V. The inset of (b) shows integrated charge density ( $Q_a$ ) for the samples.

To quantitatively compare the electrochromic properties of Ti and Ti–W ONTs, reflectance measurements were performed. Figure 2c shows *in situ* reflectance curves obtained during the pulse potential applied between  $1.0$  and  $-0.7$  V. Compared to Ti ONTs, Ti–W ONTs yield much larger values in reflectance difference ( $\Delta R$ );  $\Delta R$  was  $0.09$  for Ti ONTs,  $0.37$  for Ti-0.2W ONTs, and  $0.61$  for Ti-9W ONTs. These findings are in line with the finding of a higher amount of protons being incorporated during the reactions from the CV measurement in Figure 2. Figure 2d shows the visually observed contrast for the different materials when the voltage is switched between  $1.0$  and  $-0.7$  V.

Repeated CV cycling was performed up to  $100$  cycles to investigate the stability of oxide nanotubes during the proton insertion/extraction processes. Figure 3a–c show the changes in reflectance difference between the bleached and colored state during the CV cycles. Up to a potential of  $-0.7$  V, the initial reflectance differences are maintained without degradation. For potentials of  $> -0.7$  V, degradation of the electrochromic effect occurs. This degradation can be attributed to partial dissolution of nanotube structure (See Figure S4). It should be noted, however, that for higher addition of WO<sub>3</sub>, such as in Ti-9W ONTs, the stability can be significantly enhanced. Figure 3d shows  $\Delta R$  as a function of bias voltage after  $100$  cycles. It is apparent that over the entire cycling voltage only a comparably low threshold potential for electrochromic switching is needed in case of Ti–W

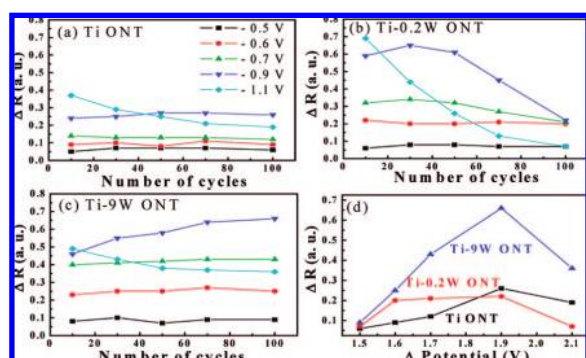


**Figure 3.** Reflectance difference obtained during  $100$  CV cycles applied between  $1.0$  V and various negative potentials for (a) Ti, (b) Ti-0.2W, and (c) Ti-9W ONTs. (d) Reflectance difference ( $\Delta R$ ) as a function of bias voltage for all samples.

ONTs. For example, for pure Ti ONTs one has to apply a negative bias of  $0.9$  V to achieve a relative color change of more than  $0.2$  in  $\Delta R$ , while only  $0.6$  V is required for comparable contrast in Ti–W ONTs. This is a feature that is highly desired in terms of power saving in practical electrochromic devices.

In summary, composite Ti–W ONTs have been successfully fabricated for the first time using TiW alloy anodization. The nanotubes show a straight wall morphology and are well vertically aligned on the substrate. Compared to Ti ONTs, the composite Ti–W ONTs showed highly improved ion insertion and electrochromic properties even when only small amounts such as  $0.2$  at% WO<sub>3</sub> are present. In particular, Ti–W ONTs have a much higher electrochromic contrast and lower onset voltage and exhibit a good cycling stability. We believe that these nanotube structures based on TiW alloy anodization can find applications, not only in electrochromic devices but also for photoelectrodes in photocatalytic devices or photoelectrochemical solar cells.

**Acknowledgment.** This work was supported by DFG and FP-6 [Ti-Nanotubes]. Y.-C.N. was supported by the Korea Research Foundation Grant (KRF-2007-357-D00064) funded by the Korean Government (MOEHRD). The authors would like to acknowledge Ulrike Marten-Jahns and Helga Hildebrand for the XRD and XPS measurements. Dr. M. Oehring at GKSS Forschungszentrum in Geesthacht is also acknowledged for providing the Ti–W alloys.

**Supporting Information Available:** Experimental details and further characterizations of the nanotubes. This information is available free of charge via the Internet at <http://pubs.acs.org/>.

## References

- (1) (a) Tsuchiya, H.; Macak, J. M.; Muller, L.; Kunze, J.; Muller, F.; Greil, P.; Virtanen, S.; Schmuki, P. *J. Biomed. Mater. Res., Part A* **2006**, *77*, 534. (b) Park, J.; Bauer, S.; von der Mark, K.; Schmuki, P. *Nano Lett.* **2007**, *7*, 1686.
- (2) (a) Albu, S. P.; Ghicov, A.; Macak, J. M.; Hahn, R.; Schmuki, P. *Nano Lett.* **2007**, *7*, 1286. (b) Macak, J. M.; Zlamal, M.; Krysa, J.; Schmuki, P. *Small* **2007**, *3*, 300.
- (3) Kongkanand, A.; Tvrdy, K.; Takechi, K.; Kuno, M.; Kamat, P. V. *J. Am. Chem. Soc.* **2008**, *130*, 4007. (b) Adachi, M.; Murata, Y.; Okada, I.; Yoshikawa, S. *J. Electrochem. Soc.* **2003**, *150*, G488.
- (4) (a) Hahn, R.; Ghicov, A.; Tsuchiya, H.; Macak, J. M.; Munöz, A. G.; Schmuki, P. *Phys. Status Solidi A* **2007**, *204*, 1281. (b) Ghicov, A.; Tsuchiya, H.; Hahn, R.; Macak, J. M.; Munöz, A. G.; Schmuki, P. *Electrochem. Commun.* **2007**, *8*, 528. (c) Ghicov, A.; Albu, S. P.; Macak, J. M.; Schmuki, P. *Small* **2008**, *4*, 1063.
- (5) (a) Kasuga, T.; Hiramatsu, M.; Hoson, A.; Sekino, T.; Niihara, K. *Langmuir* **1998**, *14*, 3160. (b) Jung, J. H.; Kobayashi, H.; van Bommel, K. J. C.; Shinkai, S.; Shimizu, T. *Chem. Mater.* **2002**, *14*, 1445. (c) Zhu, Y.; Li, H.; Koltypin, Y.; Hacoen, Y. R.; Gedanken, A. *Chem. Commun.* **2001**, 2616. (d) Kasuga, T.; Hiramatsu, M.; Hoson, A.; Sekino, T.; Niihara, K. *Langmuir* **1998**, *14*, 3160.
- (6) (a) Zwilling, V.; Darque-Ceretti, E.; Boutry-Forveille, A.; David, D.; Perrin, M. Y.; Aucouturier, M. *Surf. Interface Anal.* **1999**, *27*, 629. (b) Macak, J. M.; Tsuchiya, H.; Schmuki, P. *Angew. Chem., Int. Ed.* **2005**, *44*, 2100.
- (7) Macak, J. M.; Tsuchiya, H.; Ghicov, A.; Yasuda, K.; Hahn, R.; Bauer, S.; Schmuki, P. *Curr. Opin. Solid State Mater. Sci.* **2007**, *11*, 3.
- (8) (a) Asahi, R.; Morikawa, T.; Ohwaki, T.; Aoki, K.; Taga, Y. *Science* **2001**, *293*, 269. (b) Anpo, M.; Takeuchi, M. *J. Catal.* **2003**, *216*, 505. (c) Ghicov, A.; Macak, J. M.; Tsuchiya, H.; Kunze, J.; Haeublein, V.; Frey, L.; Schmuki, P. *Nano Lett.* **2006**, *6*, 1080.
- (9) (a) Liao, S.; Donggen, H.; Yu, D.; Su, Y.; Yuan, G. *J. Photochem. Photobiol., A* **2004**, *168*, 7. (b) Dhananjayan, M. R.; Mielczarski, E.; Thampi, K. R.; Buffat, Ph.; Bensimon, M.; Kulik, A.; Mielczarski, J.; Kiwi, J. *J. Phys. Chem. B* **2001**, *105*, 12046. (c) Li, X. Z.; Li, F. B.; Yang, C. L.; Ge, W. K. *J. Photochem. Photobiol., A* **2001**, *141*, 7.
- (10) (a) Pan, J. H.; Lee, W. I. *Chem. Mater.* **2006**, *18*, 847. (b) Keller, V.; Bernhardt, P.; Garin, F. *J. Catal.* **2003**, *215*, 129.
- (11) De Tacconi, N. R.; Chenthamarakshan, C. R.; Wouters, K. L.; MacDonnell, F. M.; Rajeshwar, K. *J. Electroanal. Chem.* **2004**, *566*, 249.
- (12) (a) Lee, S.-H.; Deshpande, R.; Parilla, P. A.; Jones, K. M.; To, B.; Mahan, A. H.; Dillon, A. C. *Adv. Mater.* **2006**, *18*, 763. (b) Deb, S. K. *Sol. Energy Mater. Sol. Cells* **2008**, *92*, 245.
- (13) (a) Tsuchiya, H.; Macak, J. M.; Sieber, I.; Taveira, L.; Ghicov, A.; Sirotna, K.; Schmuki, P. *Electrochem. Commun.* **2005**, *7*, 295. (b) Berger, S.; Tsuchiya, H.; Ghicov, A.; Schmuki, P. *Apply. Phys. Lett.* **2006**, *88*, 203119.

JA807106Y